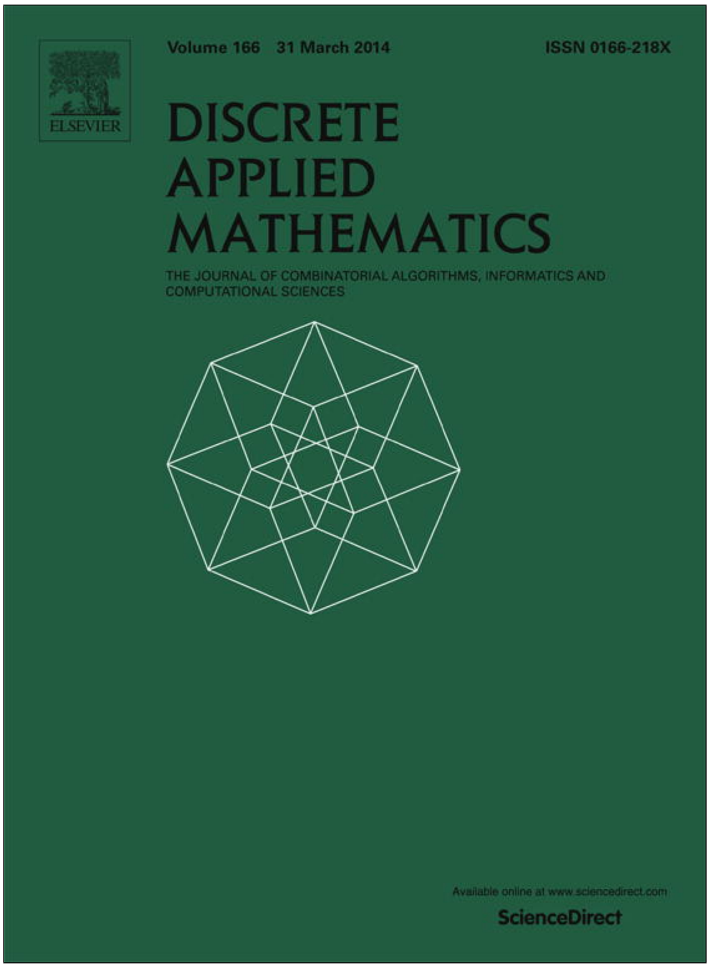
Volume 166 31 March 2014
ISSN 0166-218X
ELSEVIER
DISCRETE
APPLIED
MATHEMATICS
THE JOURNAL OF COMBINATORIAL ALGORITHMS, INFORMATICS AND COMPUTATIONAL SCIENCES
Available online at www.sciencedirect.com
ScienceDirect

Discrete Applied Mathematics 166 (2014) 141–158

Contents lists available at ScienceDirect

Discrete Applied Mathematics

journal homepage: www.elsevier.com/locate/dam

Dense bipartite circulants and their routing via rectangular twisted torus

Pranava K. Jha *

Department of Computer Science, St. Cloud State University, 720 Fourth Ave. S., St. Cloud, MN 56301-4498, United States

ARTICLE INFO

Article history:
Received 12 November 2012
Received in revised form 3 July 2013
Accepted 27 September 2013
Available online 24 October 2013

Keywords:
Circulant graphs
Rectangular twisted torus
Fault tolerance
Multiprocessor interconnection
Network topology
Graphs and networks

ABSTRACT

Whereas the maximum number of vertices in a four-regular circulant of diameter a is $2a^2 + 2a + 1$, the bound turns out to be $2a^2$ if the condition of bipartiteness is imposed. Tzvieli presented a family of $\psi(a)$ such dense bipartite circulants on $2a^2$ vertices for each $a \geq 3$, where $\psi(a)$ denotes the number of positive integers less than or equal to $\lfloor \frac{1}{2}(a-1) \rfloor$ that are coprime with a. The present paper shows that each of those graphs is obtainable from the $2a \times a$ rectangular twisted torus by appropriately trading a maximum of $2a$ edges for as many new edges. The underlying structural similarity between the two graphs leads to a simple intuitive routing algorithm for the circulants. The result closely parallels the routing in dense nonbipartite circulants on $2a^2 + 2a + 1$ vertices. Additional results include a set of vertex-disjoint paths between every pair of distinct vertices in the circulants, and a proof that the $2a \times a$ rectangular twisted torus itself is probably not a circulant.

1. Introduction and preliminaries

The *circulant graphs*, which we formally define below, constitute a subfamily of Cayley graphs [16]. They possess a number of attractive properties that render them fit for applications in areas such as distributed systems, VLSI, parallel machines and perfect codes [4,6,7,22,23]. Some of their welcome features include high connectivity, high symmetry and a rich cycle structure, which together lead to a very high degree of fault tolerance. Accordingly, they have been a topic of extensive research in engineering, computer science and mathematics for long [5,16,29].

Routing is the process of selecting path(s) in a graph/network along which to send the traffic [26]. It is a vital component of all networks. Unfortunately, the associated problem of finding a shortest path between two vertices in a circulant is NP-hard [9]. This is also because the graph admits a very compact representation leading to a small input size. A related aberration is that $dia\big(\mathcal{C}_n(1,\ s)\big)$ is not monotone in n for a fixed s [12]. This is to be contrasted with the hypercube and the torus in which a shortest path is traceable fairly quickly and intuitively. Not surprisingly, the problem of routing is crucial in the study of circulants [11,32].

For a given positive integer $a \geq 3$, a four-regular circulant of diameter a may have a maximum of $2a^2+2a+1$ vertices [3]. Indeed, such a dense circulant (which is necessarily nonbipartite) is known to exist for a long time, and it has been a topic of deep research [3–5,16,19]. See Martinez et al. [25] for recent results on its routing algorithms and implementation issues.

If the condition of bipartiteness is imposed, then the maximum number of vertices in a four-regular circulant of diameter a turns out to be $2a^2$ [14]. Again, such dense bipartite circulants are known to exist. In particular, Tzvieli [30] presented a family of $\psi(a)$ bipartite circulants on $2a^2$ vertices for each $a \geq 3$, where $\psi(a)$ denotes the number of positive integers less than or equal to $\lfloor \frac{1}{2}(a-1) \rfloor$ that are coprime with a. A major finding of this paper is that each such graph is obtainable from the $2a \times a$ *rectangular twisted torus* (RTT), which we formally define below, by appropriately trading a maximum of $2a$ edges for as many new edges. That, in turn, leads to a simple intuitive *routing algorithm* in respect of those graphs.

* Tel.: +1 3203083073; fax: +1 3203084269.
E-mail addresses: pkjha@stcloudstate.edu, pkjha384@hotmail.com.

0166-218X/$ – see front matter © 2013 Elsevier B.V. All rights reserved.
http://dx.doi.org/10.1016/j.dam.2013.09.021

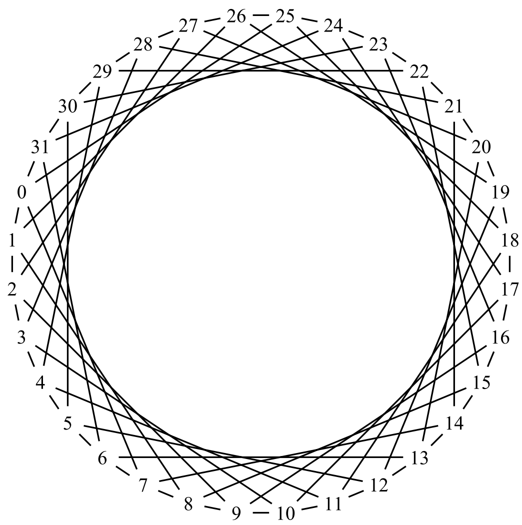

Fig. 1. The circulant $\mathcal{C}_{32}(1,\ 7)$.

Additional results include a set of vertex-disjoint paths between every pair of distinct vertices in the circulants, and a proof that the $2a \times a$ rectangular twisted torus itself is probably not a circulant.

In a closely related study, Beivide et al. [3] earlier presented a four-regular circulant $\mathcal{C}_n(b-1, b)$ on n vertices for each $n \geq 6$, where $b = \lceil \sqrt{n/2} \rceil$. The graph, known also as a *midimew network*, is such that its diameter and the average (shortest) distance are the least among all four-regular graphs on as many vertices. It turns out that the circulants in the present paper share those characteristics, hence they may be viewed as their bipartite counterparts.

1.1. Basic definitions

When we speak of a graph G, we mean a finite, simple, undirected and connected graph. Let $dist(u, v)$ denote the (shortest) distance between u and v, where the underlying graph will be clear from the context. Next, let $dia(G)$ represent the *diameter* of G, i.e., the maximum of the distances between any two vertices in G. Vertices that are at a distance of $dia(G)$ from u are called *diametrical* relative to u. We employ the terms *vertex* and *node* as synonyms. For missing details, see Hammack et al. [13].

Let P_m denote a *path* on m vertices, and C_n a *cycle* on n vertices, where $m \geq 1$ and $n \geq 3$. The *Cartesian product* $G \square H$ of graphs $G = (V, E)$ and $H = (W, F)$ is defined as follows: $V(G \square H) = V \times W$ and $E(G \square H) = \{\{(a, x), (b, y)\}: \{a, b\} \in E$ and $x = y$, or $\{x, y\} \in F$ and $a = b\}$. See Fig. 2(i) for $P_8 \square P_4$.

Let n, r and s be positive integers, where $n \geq 6$, and $1 \leq r < s < \lfloor n/2 \rfloor$. A *four-regular circulant graph* $\mathcal{C}_n(r, s)$ consists of the vertex set $\{0, \ldots, n-1\}$ and the edge set $\{\{i,\ i \pm r\}, \{i,\ i \pm s\} : 0 \leq i \leq n-1\}$, where $i \pm r$ and $i \pm s$ are each modulo n. A circulant $\mathcal{C}_n(r, s)$ with $r = 1$ is also known as a chordal ring or a double-loop graph in the literature [14,28]. Meanwhile $\mathcal{C}_{32}(1,\ 7)$ appears in Fig. 1, and Proposition 1.1 states some well-known characteristics of a four-regular circulant.

Proposition 1.1 *([27,15])*.

1. $\mathcal{C}_n(r,\ s)$ *is connected if and only if* $\gcd(n, r, s) = 1$.
2. $\mathcal{C}_n(r,\ s)$ *is bipartite if and only if* n *is even, and* r *and* s *are both odd.*
3. $\mathcal{C}_n(r,\ s)$ *is isomorphic to* $\mathcal{C}_n(r,\ n-s)$.
4. *If* $\gcd(r, n) = 1$, *then* $\mathcal{C}_n(r, s)$ *is isomorphic to* $\mathcal{C}_n(1, r^{-1}s \mod n)$, *where* r^{-1} *is the multiplicative inverse of* r *relative to* n.
5. *If* $\gcd(t, n) = 1$, *then* $\mathcal{C}_n(r,\ s)$ *is isomorphic to* $\mathcal{C}_n(rt \mod n, st \mod n)$. ■

1.2. Rectangular twisted torus

The $2a \times a$ RTT is an alternative to the $2a \times a$ *torus*, the latter being representable as $C_{2a} \square C_a$. The vertex set of the RTT is given by $\{(i,\ j) :\ 0 \leq i \leq 2a-1$ and $0 \leq j \leq a-1\}$, while the edge set consists of the following:

- $\{(i, j), (i+1, j)\}$: $0 \leq i \leq 2a-2$ and $0 \leq j \leq a-1$, called the "horizontal" edges
- $\{(i, j), (i, j+1)\}$: $0 \leq i \leq 2a-1$ and $0 \leq j \leq a-2$, called the "vertical" edges
- $\{(0, j), (2a-1, j)\}$: $0 \leq j \leq a-1$, called the "wrap-around" edges, and
- $\{(i, 0), (i+a, a-1)\}$: $0 \leq i \leq 2a-1$, called the "twisted" edges

where the arithmetic is modulo $2a$ in the first coordinate and modulo a in the second. This graph is bipartite, four-regular and nonplanar. Further, its diameter is equal to a [10], and it is obtainable from $P_{2a} \square P_a$ by introducing the "wrap-around" edges and the "twisted" edges. Graphs $P_8 \square P_4$ and 8×4 RTT appear in Fig. 2.

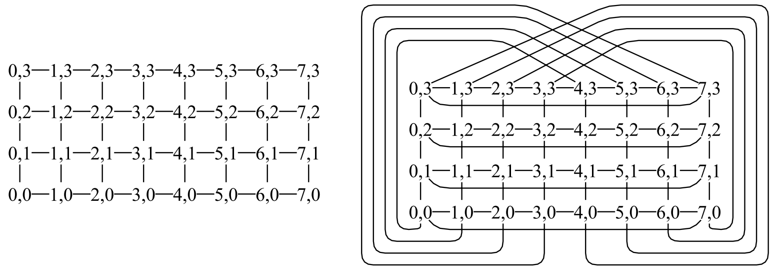

(i) (ii)

Fig. 2. (i) $P_8 \square P_4$ and (ii) 8×4 RTT.

The motivation for the RTT comes from a potential improvement to the existing topologies built around a 2D/3D torus currently in use by HP, Cray, IBM, etc. [10]. (Whereas a 2D torus is representable as $C_m \square C_n$, a 3D torus is representable as $C_m \square C_n \square C_p$ for some positive m, n and p.) Meanwhile the idea of twisting one of the two dimensions of a 2D torus earlier appeared in ILLIAC IV during 1970s [7].

Lemma 1.2 (*Alspach [1]*)**.** *The* $2a \times a$ *RTT is a Cayley graph on an abelian group.*

Proof. Consider the following mappings α and β from the vertex set of this graph to itself:

1. $\alpha(i, j) = (i + 1, j)$, and
2. $\beta(i, j) = \begin{cases} (i, j+1), & 0 \le j \le a-2 \\ (i+a, 0), & j = a-1. \end{cases}$

It is easy to see that α and β are well-defined automorphisms, and they generate a vertex-transitive group. Also, they commute under composition, so they generate an abelian transitive group. Accordingly, the $2a \times a$ RTT is a Cayley graph on the group generated by α and β. ■

It follows that the RTT is vertex transitive, i.e., for any two vertices, there exists an automorphism, which maps one to the other. Further, it is edge decomposable into Hamiltonian cycles [20].

A natural question arises: Is the $2a \times a$ RTT itself a circulant graph? Results in Section 6 suggest that the answer is probably negative.

1.3. State of the art

The circulant graphs enjoy a rich literature by virtue of their applications in parallel machines, distributed systems, VLSI, etc. Alspach and Parsons [2] addressed their isomorphism while Boesch and Tindell [5] examined their connectivity, and Heuberger [15] characterized their planarity and colorability. Further, Broere and Hattingh [8] studied the circulants that survive the stress of various product operations. See Tang et al. [29] for recent results and a hierarchy of progressively restricted classes of circulants.

Toward finding a shortest path in a circulant, Wong and Coppersmith [31] presented a geometrical approach in which a minimum distance diagram is constructed leading to a tessellation of the plane. For related results, see the survey articles by Bermond et al. [4] and Hwang [19].

Among various circulants, those of degree four are especially useful, since most of them have a torus-like structure. Issues relating to their interconnection schemes, optimal layouts, broadcasting, etc., have been examined at length [3,14,21]. See Nicoloso and Pietropaoli [28] for an algorithm to test whether or not two such graphs are isomorphic. The following result is relevant in the present study.

Lemma 1.3. *If* $a \ge 3$ *and* $1 \le k \le \lfloor \frac{1}{2}(a-1) \rfloor$, *then* $\mathcal{C}_{2a^2}(1,\ 2ka-1)$ *is isomorphic to* $\mathcal{C}_{2a^2}(1,\ 2ka+1)$.

Proof. Note that $2ka + 1$ is relatively prime to $2a^2$. Indeed, $(2ka+1)^{-1} = 2a^2 - 2ka + 1$. By Proposition 1.1(5), $\mathcal{C}_{2a^2}(1,\ 2ka-1) \cong \mathcal{C}_{2a^2}\big(2ka+1 \bmod 2a^2,\ ((2ka+1)(2ka-1)) \bmod 2a^2\big)$. Now, $2ka+1 < 2a^2$, and $(2ka+1)(2ka-1) = 4k^2a^2 - 1$ that reduces to $2a^2 - 1$ modulo $2a^2$. Therefore, $\mathcal{C}_{2a^2}(1,\ 2ka-1) \cong \mathcal{C}_{2a^2}(2ka+1,\ 2a^2-1)$. Next, $(2a^2-1)^{-1} = 2a^2-1$ relative to $2a^2$. By Proposition 1.1(4), $\mathcal{C}_{2a^2}(2ka+1,\ 2a^2-1) \cong \mathcal{C}_{2a^2}\big(1,\ ((2ka+1)(2a^2-1)^{-1}) \bmod 2a^2\big)$ that is $\mathcal{C}_{2a^2}\big(1,\ ((2ka+1)(2a^2-1)) \bmod 2a^2\big)$ that is $\mathcal{C}_{2a^2}\big(1,\ 2a^2-(2ka+1)\big)$, which itself is isomorphic to $\mathcal{C}_{2a^2}(1,\ 2ka+1)$, cf. Proposition 1.1(3). ■

Diameter of a four-regular circulant: The diameter of a graph being an important measure associated with the point-to-point transmission delay in the worst case, it is natural to look out for a circulant whose diameter is as small as possible. To that end, Boesch and Wang [6] showed that $dia\big(\mathcal{C}_n(r, s)\big)$ is greater than or equal to the least d such that $(d+1)^2 + d^2 \ge n$. Hence the following lower bound:

Theorem 1.4 *([6]). If $n \geq 6$, and $1 \leq r < s < \lfloor n/2 \rfloor$, then* $dia\big(\mathcal{C}_n(r,s)\big) \geq \left\lceil \frac{1}{2}\big(-1+\sqrt{2n-1}\big)\right\rceil$. ■

A circulant is said to be *optimal* if it has the least diameter among all such graphs of the same order.

Vertex-disjoint paths: Consider a set $\{P_{i_1}, \ldots, P_{i_k}\}$ of k simple paths between two distinct vertices x and y in a graph, where the paths themselves are vertex-disjoint, i.e., no two of them have any vertex in common except for the end nodes.

The existence of vertex-disjoint paths between every pair of distinct vertices in a graph lends strength to it. For example, communication may be speeded up using disjoint paths, and alternative routes may be found in the event of a node failure or edge failure [17,18]. It is expected that k is as large as possible and $\max\{|P_{i_1}|, \ldots, |P_{i_k}|\}$ is as small as possible.

What follows: Whereas Section 2 traces shortest paths between two vertices in the RTT, Section 3 presents the central results leading to the main theorem in respect of the family of optimal bipartite circulants on $2a^2$ vertices. Section 4 deals with L-shaped layouts of the graphs in the plane, and Section 5 traces vertex-disjoint paths in the RTT that are inherited by the circulants. That the graphs thus constructed and the RTT are mutually nonisomorphic appears in Section 6. Finally Section 7 summarizes the findings with certain concluding remarks.

2. Shortest paths in the RTT

Unlike a grid or a torus, the RTT is not amenable to a simple expression as far as shortest paths are concerned. We present an algorithm for that purpose that relies on the distance-wise partition of the graph.

The diameter of the $2a \times a$ RTT being equal to a [10], let $\{V_0, \ldots, V_a\}$ be its vertex partition, where V_j consists of vertices at a distance of j from $(0, 0)$, $0 \leq j \leq a$. We refer to the vertices in V_j to be at the jth level. The graph being bipartite, nodes at the same level are necessarily nonadjacent. It is known that $|V_0| = 1$, $|V_j| = 4j$ for $1 \leq j \leq a-1$, and $|V_a| = 2a-1$ [10,24]. An explicit construction of the partition follows.

For $1 \leq j \leq a$, let A_j consist of vertices at a distance of j from $(0, 0)$ relative to the grid $P_{2a}\Box P_a$; let B_j consist of vertices at a distance of $j-1$ from $(2a-1, 0)$ relative to the same grid; and let C_j consist of vertices at a distance of $j-1$ from $(a, a-1)$ relative to the same grid. Accordingly,

$$A_j = \begin{cases} \{(i, j-i) : 0 \leq i \leq j\} & 0 \leq j \leq a-1 \\ \{(i, j-i) : 1 \leq i \leq j\} & j = a. \end{cases}$$

$$B_j = \begin{cases} \{(2a-j+i, i) : 0 \leq i \leq j-1\}, & 1 \leq j \leq a-1 \\ \{(2a-j+i, i) : 1 \leq i \leq j-1\}, & j = a. \end{cases}$$

$$C_j = L_j \cup R_j, \quad \text{where}$$

$$L_j = \{(a-j+i, a-i) : 1 \leq i \leq j-1\} \quad 2 \leq j \leq a-1$$

$$R_j = \{(a+i, a+i-j) : 0 \leq i \leq j-1\} \quad 1 \leq j \leq a-1.$$

It turns out that $V_j = A_j \cup B_j \cup C_j$, $1 \leq j \leq a$. The following statements are in order:

- For $1 \leq j \leq a-1$, the sets A_j, B_j and C_j are mutually disjoint; further, $|A_j| = j+1$, $|B_j| = j$ and $|C_j| = 2j-1$, so $|V_j| = |A_j \cup B_j \cup C_j| = 4j$.
- $V_a = \{(i, a-i) : 1 \leq i \leq a\} \cup \{(i, i-a) : a+1 \leq i \leq 2a-1\}$, so there are $2a-1$ diametrical vertices.

Fig. 3(i) depicts the foregoing construction in respect of the 14×7 RTT while Fig. 3(ii) illustrates the *level diagram*. (The arrows highlight the progress of the shortest paths toward the diametrical vertices, which themselves appear within "rectangles".) Not all edges appear in Fig. 3(ii).

Algorithm 1 computes the distance and a shortest path between vertices $(0, 0)$ and (i, j) in the RTT. Its correctness follows from the foregoing discussion. Vertex transitivity ensures that it is easily adaptable for a source other than $(0, 0)$, cf. Lemma 1.2. Interestingly, it is equally applicable to the circulants that are forthcoming in the next section.

It is clear that Algorithm 1 runs in time that is linear in the length of a shortest path being sought, so it is optimal. More precisely, its running time is $O(a)$, since diameter of the RTT is equal to a.

3. Transforming the RTT into circulants

We show in this section that the circulant $\mathcal{C}_{2a^2}(1,\ 2ka-1)$ is obtainable from the $2a \times a$ RTT by trading a maximum of $2a$ edges for as many new edges. The method of attack is as follows:

- Set up a bijection from the vertex set of the RTT to that of the circulant, and examine the vertices and their adjacencies in the light of the mapping.
- Isolate those edges that come in the way of the graph being isomorphic to the circulant – call them "incompatible" edges – and replace them by as many new edges so that the resulting graph is the circulant.

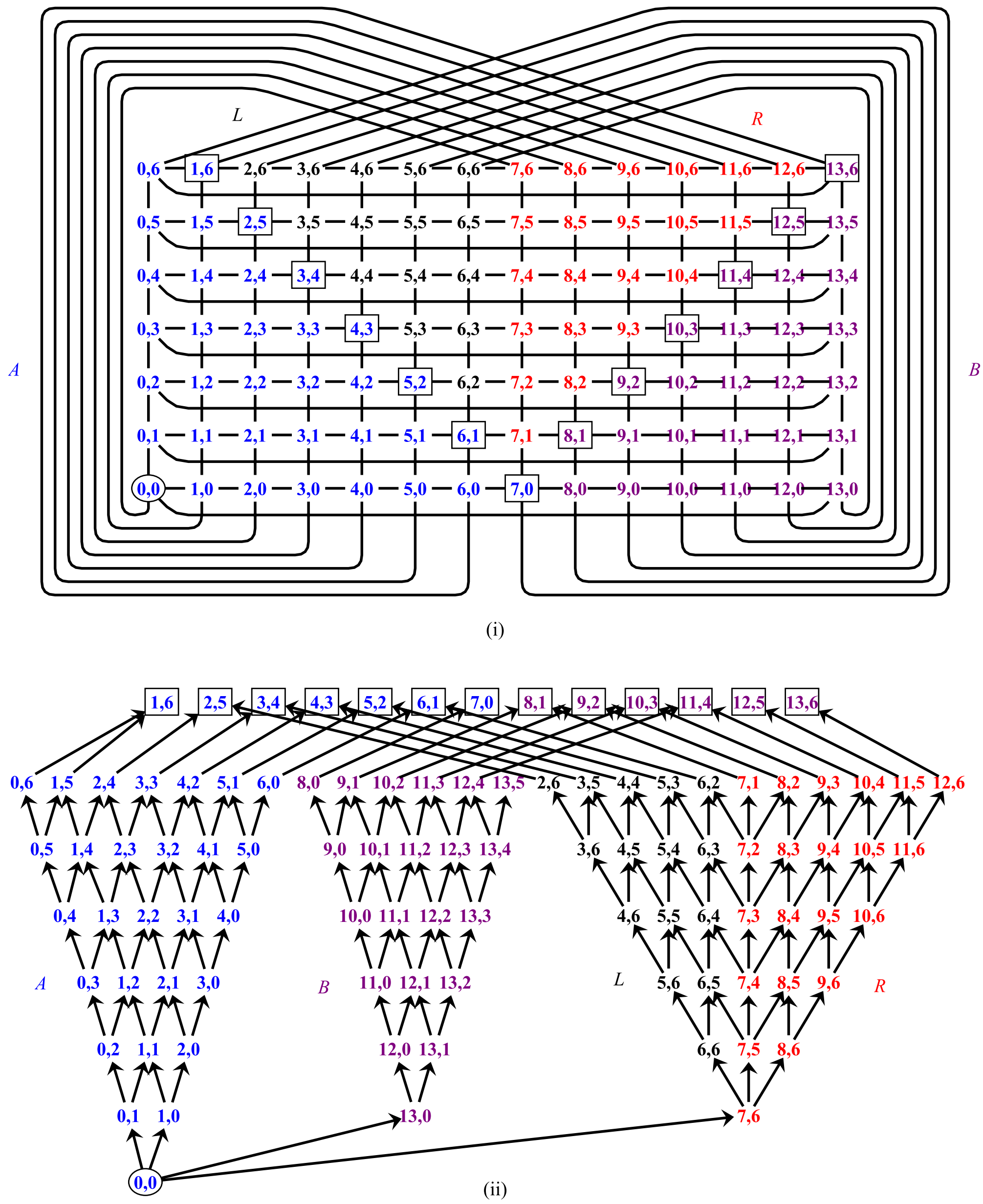

Fig. 3. 14 × 7 RTT and its level diagram.

Algorithm 1 A shortest $(0, 0) - (i, j)$ path in the RTT

Require: $0 \le i \le 2a - 1$ and $0 \le j \le a - 1$.
  if $(i + j \le a)$ **then**
    the distance is $i + j$ // Sets $A_0, \ldots, A_a$
    and a shortest path is $(0, 0) - (1, 0) - \cdots - (i, 0) - (i, 1) - \cdots - (i, j)$;
  else if $(i - j \ge a)$ **then**
    the distance is $2a - (i - j)$ // Sets $B_1, \ldots, B_a$
    and a shortest path is $(0, 0) - (2a - 1, 0) - (2a - 2, 0) - \cdots - (i, 0) - (i, 1) - \cdots - (i, j)$;
  else if $(i < a)$ **then**
    the distance is $2a - (i + j)$ // Sets $L_1, \ldots, L_{a-1}$
    and a shortest path is $(0, 0) - (a, a - 1) - (a - 1, a - 1) - \cdots - (i, a - 1) - (i, a - 2) - \cdots - (i, j)$;
  else
    the distance is $i - j$ // Sets $R_1, \ldots, R_{a-1}$
    and a shortest path is $(0, 0) - (a, a - 1) - (a + 1, a - 1) - \cdots - (i, a - 1) - (i, a - 2) - \cdots - (i, j)$;
  end if

Table 1
Nomenclature.

a:	Parameter of the $2a \times a$ rectangular twisted torus (RTT) and the circulants $\mathcal{C}_{2a^2}(1,\ 2ka-1)$, $a \geq 3$
n:	Number of vertices in the RTT/circulants, $n = 2a^2$
k:	Parameter of the circulants, $1 \leq k \leq \lfloor \frac{1}{2}(a-1) \rfloor$ with $\gcd(a, k) = 1$
k^{-1}:	Multiplicative inverse of k relative to a
s:	Parameter of the circulants, $s = 2ka - 1$
f:	Bijection from $\{0, \ldots, 2a-1\} \times \{0, \ldots, a-1\}$ to $\{0, \ldots, 2a^2-1\}$
S_i:	Sets in the partition of $\{0, \ldots, 2a^2-1\}$, $\lvert S_i \rvert = 2a$ $0 \leq i \leq a-1$

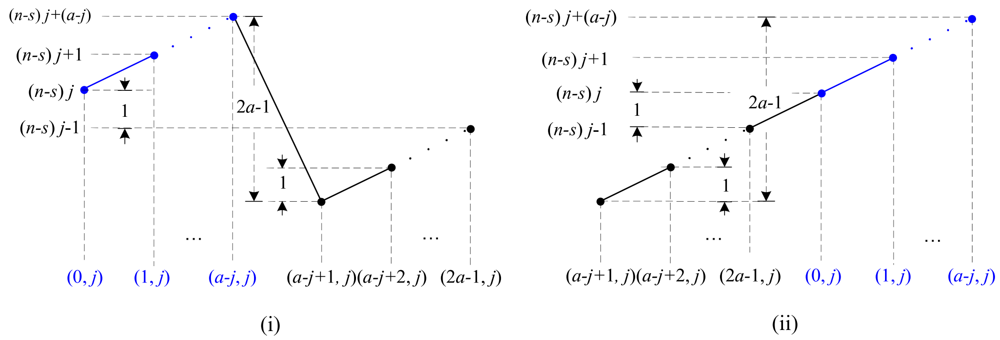

Fig. 4. $f(*, j)$ vs. $(*, j)$ in the light of Eq. (1).

See Table 1 for a set of terms that will be frequently used in the rest of the paper. It is easy to see that $s < \frac{1}{2}n < n-s < n$. Further, s is coprime with each of a, k and n, and the following inequalities hold:

$$a \text{ odd}: \begin{cases} 2a-1 \leq s \leq a^2-(a+1) \\ a^2+(a+1) \leq (n-s) \leq 2a^2-(2a-1). \end{cases}$$

$$a \text{ even}: \begin{cases} 2a-1 \leq s \leq a^2-(2a+1) \\ a^2+(2a+1) \leq (n-s) \leq 2a^2-(2a-1). \end{cases}$$

Lemma 3.1. *For* $0 \leq i \leq a-1$, $\big((a-i)+(n-s)i\big) \bmod n$ *is equal to* $(2m+1)a$, *for some* $m \in \{0, \ldots, a-1\}$.

Proof. The claim is immediate for $i = 0$, so let $i \geq 1$, and note that $(a-i)+(n-s)i = n+a-(s+1)i = n+a-2ika$. Therefore, $\big((a-i)+(n-s)i\big) \bmod n = (-2ika+a) \bmod n$. Since n itself is a multiple of $2a$, $(-2ika+a) \bmod n$ must be as claimed. ■

Lemma 3.2. *If* $0 \leq j, m \leq a-1$ *and* $j \neq m$, *then* $\big((a-j)+(n-s)j\big) \bmod n$ *and* $\big((a-m)+(n-s)m\big) \bmod n$ *differ by a nonzero multiple of* $2a$.

Proof. Without loss of generality, let $m = j+d$, where $1 \leq d \leq a-1$. By the proof of Lemma 3.1, $\big((a-j)+(n-s)j\big) \bmod n = (-2jka+a) \bmod n$, and $\big((a-m)+(n-s)m\big) \bmod n = (-2mka+a) \bmod n$, the latter being equal to $(-2jka+a-2dka) \bmod n$. It is clear that $2dka$ is nonzero and a multiple of $2a$. Also, since $\gcd(a, k) = 1$ and $d < a$, dk itself cannot be a multiple of a, hence $2dka$ cannot be a multiple of $2a^2$. The claim follows. ■

Consider now the following mapping from the vertex set of the $2a \times a$ RTT to $\{0, \ldots, 2a^2-1\}$:

$$f(u, v) = \begin{cases} \big(u+(n-s)v\big) \bmod n, & u+v \leq a \\ \big(u+(n-s)v-2a\big) \bmod n, & u+v > a \end{cases} \tag{1}$$

where $0 \leq u \leq 2a-1$ and $0 \leq v \leq a-1$. The mapping is clearly well-defined.

Based on the vertex partition in Section 2, let Region A denote the set of vertices in the RTT satisfying $u+v \leq a$, and let Region B/C denote the set of the remaining vertices. ($\lvert A \rvert = \frac{1}{2}a(a+3)$ and $\lvert B/C \rvert = \frac{1}{2}3a(a-3)$.)

The following is a key result in the present study.

Lemma 3.3. *The mapping* f *in Eq.* (1) *is a bijection.*

Proof. First note that $f(i, 0) = i$, $0 \leq i \leq a$, and $f(a+i, 0) = n+i-a$, $1 \leq i \leq a-1$. For $j \geq 1$, Fig. 4(i) presents the working of f on vertices in the jth row of the RTT. Observe that

- $f(0, j) < f(1, j) < \cdots < f(a-j, j)$
- $f(a-j+1, j) = f(a-j, j) - (2a-1)$

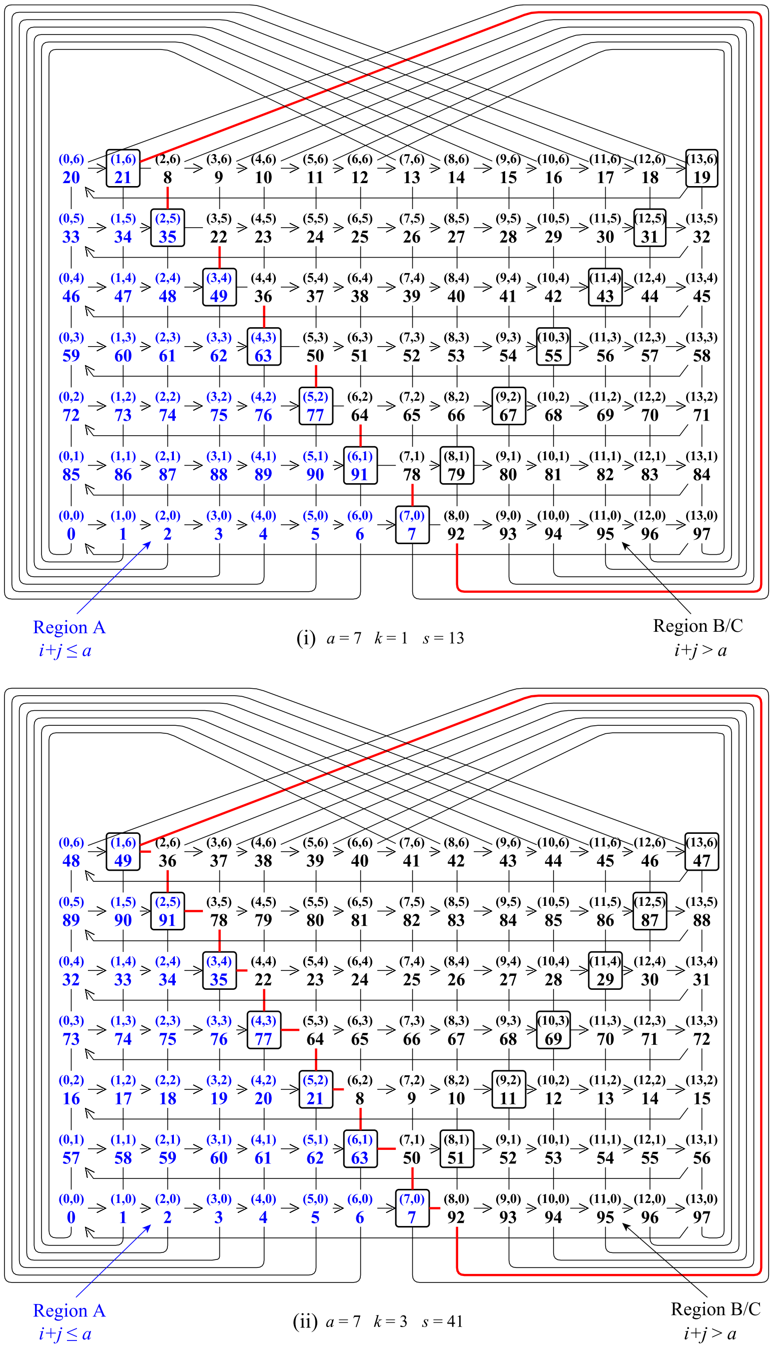

Fig. 5. The 14×7 RTT in the light of Eq. (1).

- $f(a-j+1, j) < f(a-j+2, j) < \cdots < f(2a-1, j)$, and
- $f(0, j) = 1 + f(2a-1, j)$.

Fig. 4(ii) reorganizes the snapshot so that the integer labels themselves are in the ascending order:

$$f(a-j+1, j) < f(a-j+2, j) < \cdots < f(2a-1, j) < f(0, j) < \cdots < f(a-j, j).$$

Lemma 3.1 ensures that the illustrations themselves are well-defined. (Expressions along the ordinate must be reduced modulo n.) Note that the sequence of labels in Fig. 4(ii) constitutes a run of $2a$ consecutive integers. (For $j = 0$, the labels are consecutive modulo n.) To complete the proof, therefore, it suffices to show that $\big(f(a-j, j) - f(a-m, m)\big) \bmod n$ is a nonzero multiple of $2a$, where $j \neq m$. To that end, Lemma 3.2 fits the bill. ■

Fig. 5(i) and (ii), respectively, illustrate Lemma 3.3 in respect of (i) $a = 7, k = 1, s = 13$, and (ii) $a = 7, k = 3, s = 41$. Each node consists of the ordered pair (i, j) and $f(i, j)$. Arrows have been assigned to $2a - 1$ horizontal edges in each row to highlight the run of $2a$ consecutive node labels. The relevance of the "solid" lines will be clear following the proof of Lemma 3.6.

Lemma 3.4. *For* $0 \le i \le a-1$:

$$f(a-i, i) = \big(2ai(a-k)+a\big) \bmod n.$$
$$f(a+1-i, i) = \big(2ai(a-k)-a+1\big) \bmod n.$$

Proof. Node $(a-i, i)$ being in Region A, $f(a-i,i) = \big(a-i+(n-s)i\big) \bmod n = \big(a-i+(2a^2-2ak+1)i\big) \bmod n = \big(2a^2 i - 2aik + a\big) \bmod n = \big(2ai(a-k)+a\big) \bmod n$. Further, Node $(a+1-i, i)$ being in Region B/C, $f(a+1-i,i) = \big(a+1-i+(n-s)i-2a\big) \bmod n = \big(a+1-i+(2a^2-2ak+1)i-2a\big) \bmod n = \big(2ai(a-k)-a+1\big) \bmod n$. ■

3.1. Inverse of the bijection

It is instructive to construct the inverse of the bijection f. To that end, let

- $S_0 = \{(2a-1)a+1, \ldots, 2a^2-1\} \cup \{0, \ldots, a\}$, and
- $S_i = \{(2i-1)a+1, \ldots, (2i+1)a\}$, $1 \le i \le a-1$.

It is clear that $S_0, \ldots, S_{a-1}$ constitute a partition of $\{0, \ldots, 2a^2-1\}$.

Lemma 3.5. *Vertices* $(0, j), \ldots, (2a-1, j)$ *of the RTT receive labels from the set* $S_{(-jk) \bmod a}$.

Proof. It is easy to see that the claim is valid for $j = 0$, so let $1 \le j \le a-1$. Based on the proof of Lemma 3.3, it suffices to show that $f(a-j, j)$ belongs to $S_{(-jk) \bmod a}$.

By Lemma 3.1, $f(a-j, j) = (-2jka + a) \bmod n$. Since j is less than a and $\gcd(k, a) = 1$, it is clear that $-jk$ itself cannot be a multiple of a. Let $-jk = ma + q$, where $1 \le q \le a-1$, and note that $(-2jka + a) = 2ma^2 + (2q+1)a$. Accordingly, $(-2jka + a) \bmod n$ is equal to $(2q+1)a$, since $n = 2a^2$ and $(2q+1)a < n$. Note that $(2q+1)a$ belongs to S_q that is $S_{(-jk) \bmod a}$. ■

Observe that "$j \mapsto (-jk) \bmod a$" implicit in the proof of Lemma 3.5 is a bijection from $\{0, \ldots, a-1\}$ to itself, and its inverse is given by "$j \mapsto (-jk^{-1}) \bmod a$". Algorithm 2 computes $f^{-1}(u)$, where $u \in \{0, \ldots, 2a^2-1\}$.

Algorithm 2 Calculate $f^{-1}(u)$

```
Require: 0 ≤ u ≤ 2a² − 1
  if (u ≥ 0 and u ≤ a) then
    return (u, 0);
  else if (u ≥ 2a² − (a − 1) and u ≤ 2a² − 1) then
    return (u + 2a − 2a², 0);
  else
    write u = (2i − 1)a + w,
        where 1 ≤ i ≤ a − 1 and 1 ≤ w ≤ 2a; // u ∈ S_i
    m = (−ik⁻¹) mod a;
    j = ((a − m) + w) mod 2a;
    return (j, m);
  end if
```

3.2. Transformation continued

It turns out that there are a incompatible edges in the form of a matching if $k = 1$, and $2a$ such edges in the form of a cycle if $k \ge 2$. See Fig. 6.

Lemma 3.6. 1. *Let* $k = 1$. *Except for the edges in the matching in* Fig. 6(i), *each edge* $\{(i, j), (p, q)\}$ *in the* $2a \times a$ *RTT is such that* $|f(p, q) - f(i, j)|$ *is equal to one of the following:* $1, n-1, s, n-s$.
2. *Let* $k \ge 2$. *Except for the edges in the cycle in* Fig. 6(ii), *each edge* $\{(i, j), (p, q)\}$ *in the* $2a \times a$ *RTT is such that* $|f(p, q) - f(i, j)|$ *is equal to one of the following:* $1, n-1, s, n-s$.

Proof. We first attack (2).

A horizontal edge or a vertical edge running across the two regions are excluded, and so is the twisted edge $\{(a+1, 0), (1, a-1)\}$. For the wrap-around edges and the remaining horizontal edges, the claim follows from the proof of Lemma 3.3.

If $\{(i, j), (i, j+1)\}$ is a vertical edge in Region A, then $f(i, j) = i + (n-s)j \bmod n$ and $f(i, j+1) = i + (n-s)(j+1) \bmod n$. Since $|\big(i + (n-s)j\big) - \big(i + (n-s)(j+1)\big)| = n - s$ that is positive and less than n, it follows that $|f(i, j) - f(i, j+1)|$ is equal to $n - s$ or s. The argument is similar if $\{(i, j), (i, j+1)\}$ is a vertical edge in Region B/C. We examine the remaining $2a - 1$ (twisted) edges.

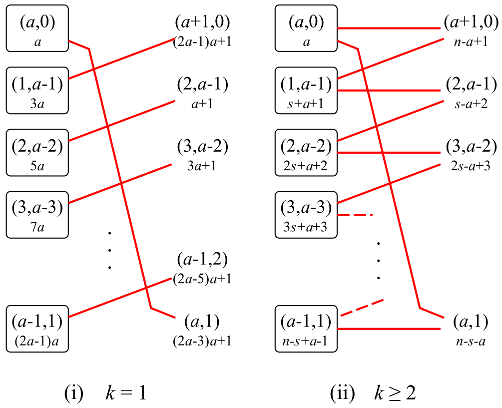

Fig. 6. Incompatible edges in the RTT.

- $\{(i,0),(i+a,a-1)\}, 0 \le i \le a-1$ (i.e., twisted edges across the two regions): $f(i,0) = i$; and $f(i+a,a-1) = \big((a+i)+(n-s)(a-1)-2a\big) \bmod n = \big((i+s)+n(a-1)-(s+1)a\big) \bmod n = \big((i+s)+n(a-1)-2ka^2\big) \bmod n = \big((i+s)+n(a-1-k)\big) \bmod n = i+s$. Accordingly, $|f(i+a,a-1)-f(i,0)| = s$.
- $\{(a,0),(0,a-1)\}$ (i.e., the twisted edge in Region A): $f(a,0) = a$; and $f(0,a-1) = (n-s)(a-1) \bmod n = \big(n(a-1)-sa+s\big) \bmod n = \big(n(a-1)-(2ka-1)a+s\big) \bmod n = \big(n(a-1)-2ka^2+a+s\big) \bmod n = \big(n(a-1-k)+a+s\big) \bmod n = a+s$. Accordingly, $|f(0,a-1)-f(a,0)| = s$.
- $\{(i,0),(i-a,a-1)\}, a+2 \le i \le 2a-1$ (i.e., twisted edges in Region B/C): $f(i,0) = (i-2a) \bmod n = n+i-2a$; and $f(i-a,a-1) = \big((i-a)+(n-s)(a-1)-2a\big) \bmod n = \big((i-a)+n(a-1)-sa+s-2a\big) \bmod n = \big(i+n(a-1)-(s+1)a+s-2a\big) \bmod n = \big(i+n(a-1)-2ka^2+s-2a\big) \bmod n = \big(n(a-1-k)+i+s-2a\big) \bmod n = i+s-2a$. Accordingly, $|f(i-a,a-1)-f(i,0)| = n-s$.

For (1), we need additionally show that $\{(i,a-i),(i+1,a-i)\}, 1 \le i \le a$, (i.e., horizontal edges running across the two regions) conform to the stated condition. (Note that $s = 2a-1$ in this case.) To that end, $f(i,a-i) = \big(i+(n-s)(a-i)\big) \bmod n = \big(i+n(a-i)-sa+si\big) \bmod n = \big(i+n(a-i)-(s+1)a+a+si\big) \bmod n = \big(i+n(a-i)-2a^2+a+si\big) \bmod n = \big(n(a-i-1)+a+(s+1)i\big) \bmod n = \big((s+1)i+a\big) \bmod n$. Further, $f(i+1,a-i) = \big(i+1+(n-s)(a-i)-2a\big) \bmod n = \big(i+1+n(a-i)-sa+si-2a\big) \bmod n = \big(i+1+n(a-i)-(s+1)a+si-a\big) \bmod n = \big(i+1+n(a-i)-2a^2+si-a\big) \bmod n = \big(n(a-i-1)+(s+1)i-a+1\big) \bmod n = \big((s+1)i-a+1\big) \bmod n$. Since $|\big((s+1)i-a+1\big)-\big((s+1)i+a\big)| = 2a-1$ that is positive and less than n, $|f(i+1,a-i)-f(i,a-i)|$ is equal to $2a-1$ or $n-(2a-1)$. ■

Note that each incompatible edge is such that one of its endpoints is of the form $(a-j,j)$ (a diametrical vertex in Region A), and the other is of the form $(a+1-j,j)$. See Fig. 5, which illustrates such edges using "solid" lines in respect of the 14×7 RTT.

The next step is to trade the incompatible edges for as many new edges so that the resulting graph is isomorphic to a circulant graph.

Lemma 3.7. *If $k = 1$, then the graph obtainable from the $2a \times a$ RTT by dropping the edges from Fig. 6(i) and adding the edges from Fig. 7(i) is isomorphic to $\mathcal{C}_{2a^2}(1,\ 2a-1)$.*

Proof. First note that there are as many edges in Fig. 7(i) as in Fig. 6(i), and the set of underlying vertices is the same in each. Further, the edges in Fig. 7(i) are new. Finally, check to see that the following hold:

- $f(a,0) = a$ and $f(2,a-1) = a+1$
- $f(a-1,1) = (2a-1)a$ and $f(a+1,0) = (2a-1)a+1$, and
- $f(j,a-j) = (2j+1)a$ and $f(j+2,a-1-j) = (2j+1)a+1$, where $1 \le j \le a-2$.

It is clear that the foregoing edge exchanges lead to $\mathcal{C}_{2a^2}(1,\ 2a-1)$. ■

Lemma 3.8. *If $k \ge 2$, then the graph obtainable from the $2a \times a$ RTT by dropping the edges from Fig. 6(ii) and adding the edges from Fig. 7(ii) is isomorphic to $\mathcal{C}_{2a^2}(1,\ 2ka-1)$.*

Proof. First recall the identities from Lemma 3.4:

1. $f(a-i,i) = \big(2ai(a-k)+a\big) \bmod n, 0 \le i \le a-1$.
2. $f(a+1-i,i) = \big(2ai(a-k)-a+1\big) \bmod n, 0 \le i \le a-1$.

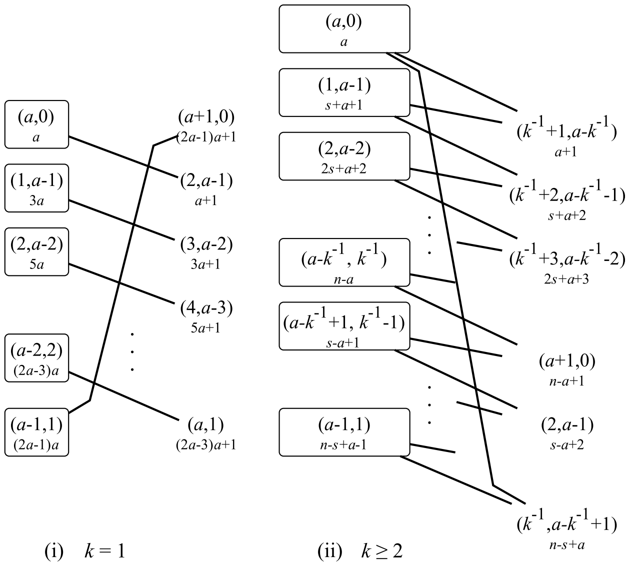

Fig. 7. New edges.

The following are obtainable from the foregoing using the fact that $kk^{-1} = ma + 1$ for some m:

3. $f(a - (k^{-1} - i), k^{-1} - i) = \big(2kai - a\big) \bmod n$.
4. $f(k^{-1} + i, a + 1 - (k^{-1} + i)) = \big(2ka(i - 1) + (a + 1)\big) \bmod n$.

The rest of the argument is similar to that in the proof of Lemma 3.7. Check to see that the labels assigned to the vertices in Fig. 7(ii) are correct, and that the difference modulo n of the labels to the endpoints of each edge is equal to one of the following: $1, n - 1, s, n - s$. ■

Fig. 8(i) and (ii) illustrate the working of Lemmas 3.7 and 3.8, respectively. The new edges appear as "dark" lines.

It is easy to see that the edge exchanges in the present line of construction are such that the distance-wise vertex distribution of the RTT (cf. Section 2) holds true in respect of the resulting circulants as well. The following observation is in order:

- Algorithm 1 (Section 2) for a shortest path between two vertices in the RTT does not make use of an incompatible edge or a new edge. Therefore, it remains valid for each circulant.

It follows that the existing results on the diameter, average distance and link utilization of the RTT (Cámara et al.'s Lemma 7 [10, p. 1768]) seamlessly carry over to each of the resulting circulants. (Link utilization is the average usage of the network links under uniform random traffic at maximum network load. It is equal to the sum of the normalized average distances per dimension, averaged among the network dimensions [10].)

In case the set of vertices of the circulant is given as $\{0, \ldots, 2a^2 - 1\}$, Algorithm 2 (Section 3.1) may be used to transform it into the vertex set of the RTT.

Lemma 3.9. *The following hold for each circulant built in this section: diameter* $= a$*; average distance* $= \frac{4a^3-1}{6a^2} \approx \frac{2a}{3}$*; and link utilization* $= 1$. ■

Observe that Lemma 3.9 achieves the lower bound on the diameter, cf. Theorem 1.4. Here is the central result of this paper.

Theorem 3.10. *For each* $a \geq 3$*, there exists a family of optimal four-regular bipartite circulants* $\mathcal{C}_{2a^2}(1, 2ka - 1)$*, each obtainable from the* $2a \times a$ *rectangular twisted torus, where* $1 \leq k \leq \lfloor \frac{1}{2}(a - 1) \rfloor$ *and* $\gcd(a, k) = 1$. ■

4. Layout of the circulants in the plane

Engineering considerations dictate that a network admit a layout that is amenable to an embedding of parallel algorithms. It turns out that every four-regular circulant admits an L-shaped embedding with wrap-around links in the 2D plane [19]. The layout itself is amenable to a plane tessellation that is useful in the design of an efficient routing algorithm relative to the given graph. Meanwhile the concept has its root in the construction of a minimum-distance diagram of a regular graph [31].

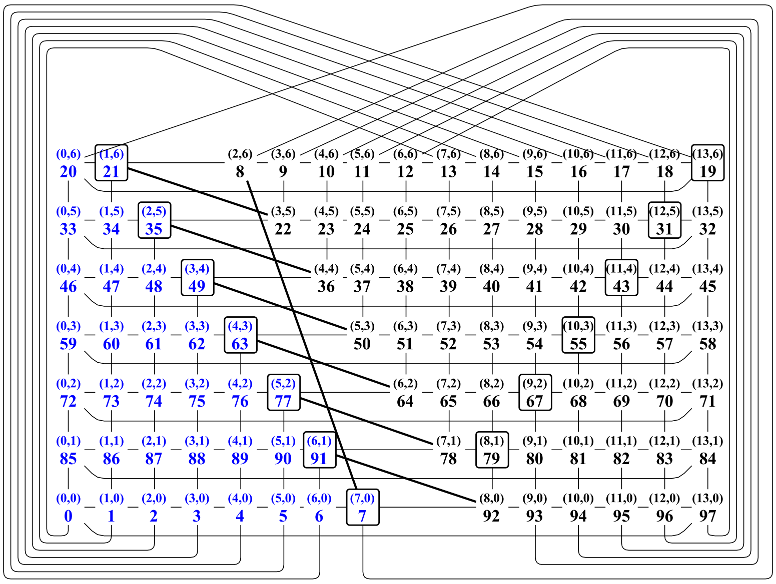

(i) $a = 7$ $k = 1$ $s = 13$

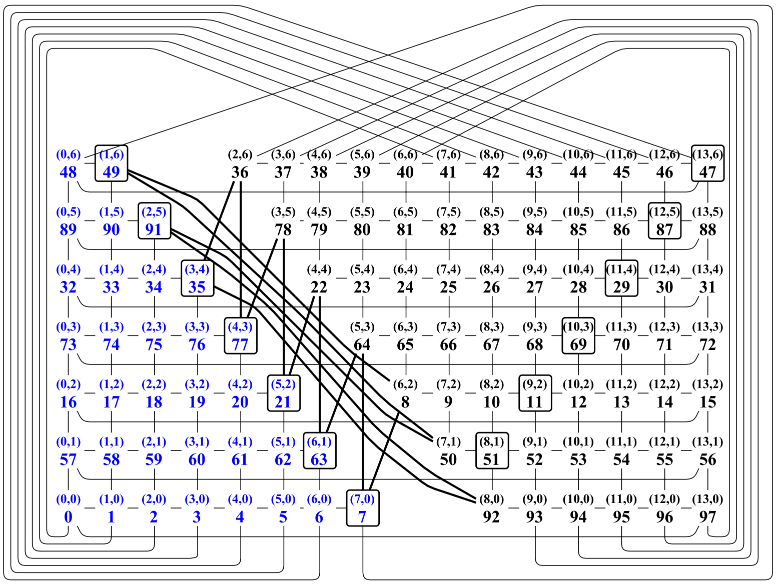

(ii) $a = 7$ $k = 3$ $s = 41$

Fig. 8. The 14 × 7 RTT transformed into (i) $\mathcal{C}_{98}(1,\ 13)$ and (ii) $\mathcal{C}_{98}(1,\ 41)$.

The arrangement for $\mathcal{C}_{2a^2}(1, 2a-1)$ is relatively easy. See Fig. 9 that illustrates this case in respect of $\mathcal{C}_{98}(1, 13)$. It is essentially a careful presentation of Fig. 8(i). A general framework of the vertex layout for this case appears in Fig. 10. (The nodes within "rectangles" are exactly those that are diametrical relative to (0, 0).)

4.1. Layout of $\mathcal{C}_{2a^2}(1, 2ka-1)$, $k \geq 2$

As in Section 3, we let $a \geq 3$, $n = 2a^2$ and $k \in \{1, \ldots, \lfloor \frac{1}{2}(a-1) \rfloor\}$ with $\gcd(a, k) = 1$. For $k \geq 2$ (in which case $a \geq 5$), it is easy to see that $k^{-1} \geq 3$. Indeed, if a is odd, then $2^{-1} = \frac{1}{2}(a+1)$ that is greater than $\lfloor \frac{1}{2}(a-1) \rfloor$. On the other hand, if a is even, then k cannot be equal to 2. A scheme for vertex layout of the graph in the plane appears in Algorithm 3 (see Figs. 11 and 12).

Aspect ratio: The *aspect ratio* of a layout is the ratio of the width and the height of the smallest enclosing rectangle. For the foregoing layouts of $\mathcal{C}_{2a^2}(1,\ 2ka-1)$, it is given by $\frac{2a-k^{-1}}{a+k^{-1}}$, which achieves its maximum of nearly two if $k^{-1} = 1$, i.e., $k = 1$. On the other hand, it reaches its minimum of a little over $\frac{1}{2}$ if k^{-1} is close to a, and that happens when a is odd and $k^{-1} = a - 2$ corresponding to $k = \frac{1}{2}(a-1)$.

See Table 2 for relative values of a and k where the objective is to achieve an aspect ratio close to unity.

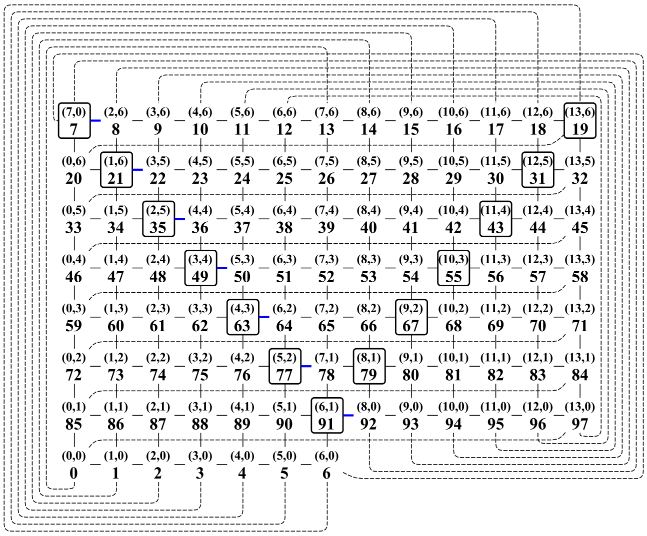

Fig. 9. L-shaped layout of $\mathcal{C}_{98}(1,\ 13)$.

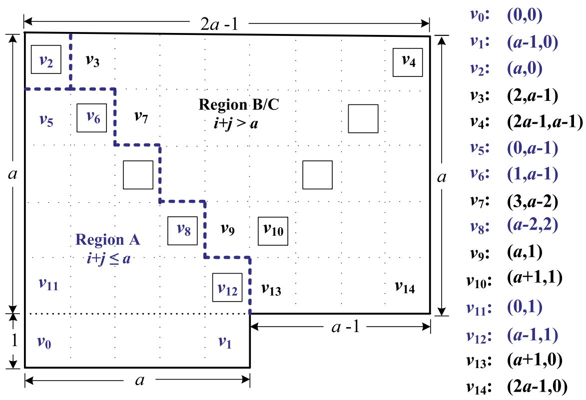

Fig. 10. A framework for layout of $\mathcal{C}_{2a^2}(1,\ 2a-1)$.

Algorithm 3 Vertex layout of $\mathcal{C}_{2a^2}(1, 2ka-1)$, $k \geq 2$

Require: $a \geq 5$ and $k \geq 2$, where $\gcd(k, a) = 1$.

Step 1: Consider the embedding of the $2a \times a$ RTT in the plane where incompatible edges have been distinguished. See Fig. 5(ii) in respect of the 14×7 RTT.

Step 2: Delete the following:

1) The incompatible edges (which include one twisted edge).
2) The wrap-around edges.
3) The twisted edges $\{(i, 0), (i+a, a-1)\}$: $0 \leq i \leq a-1$, and $\{(a+k^{-1}+i, 0), (k^{-1}+i, a-1)\}$: $0 \leq i \leq a-k^{-1}+1$. (The twisted edges that remain are: $\{(a, 0), (0, a-1)\}$, and $\{a+2+i, 0), (2+i, a-1)\}$: $0 \leq i \leq k^{-1}-3$, i.e., $k^{-1}-1$ of them.)
4) The horizontal edges $\{(k^{-1}-1, j), (k^{-1}, j)\}$: $a-k^{-1}+2 \leq j \leq a-1$. (There are $k^{-1}-2$ of them.)

Step 3: Reorganize the layout from Step 2, so Region A and Region B/C from the initial partition form two separate blocks.

Step 4: Carefully juxtapose the two blocks so that they are left-justified and "vertically" aligned, and the vertex $(a, 0)$ is immediately to the left of $(k^{-1}+1, a-k^{-1})$. Finally piece them together using the new edges.

Step 5: Introduce the remaining valid edges. Fig. 11 presents the final layout of $\mathcal{C}_{98}(1,\ 41)$ where the new edges appear prominently while Fig. 12 depicts a general framework for that purpose.

5. Vertex-disjoint paths in the RTT

This section presents certain vertex-disjoint paths between every pair of distinct vertices in the RTT that directly map into analogous paths in $\mathcal{C}_{2a^2}(1, 2ka-1)$.

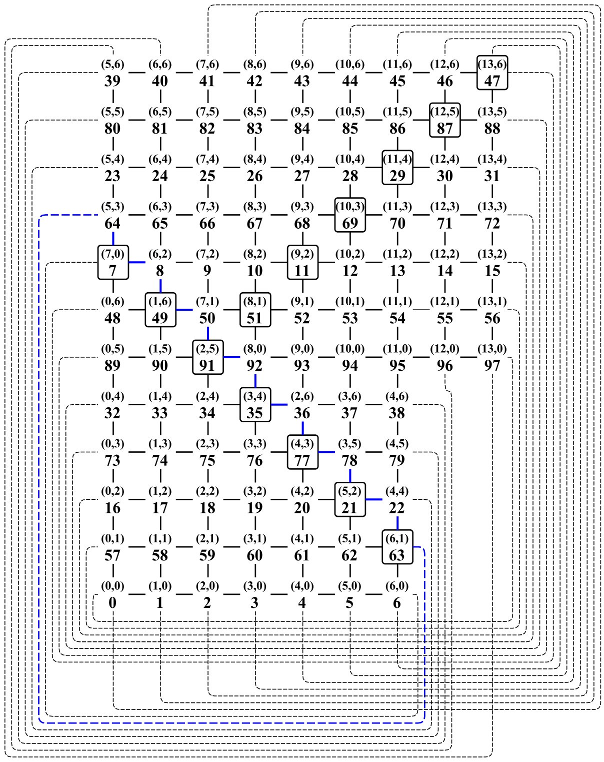

Fig. 11. Layout of $\mathcal{C}_{98}(1, 41)$ (Step 5 of Algorithm 3).

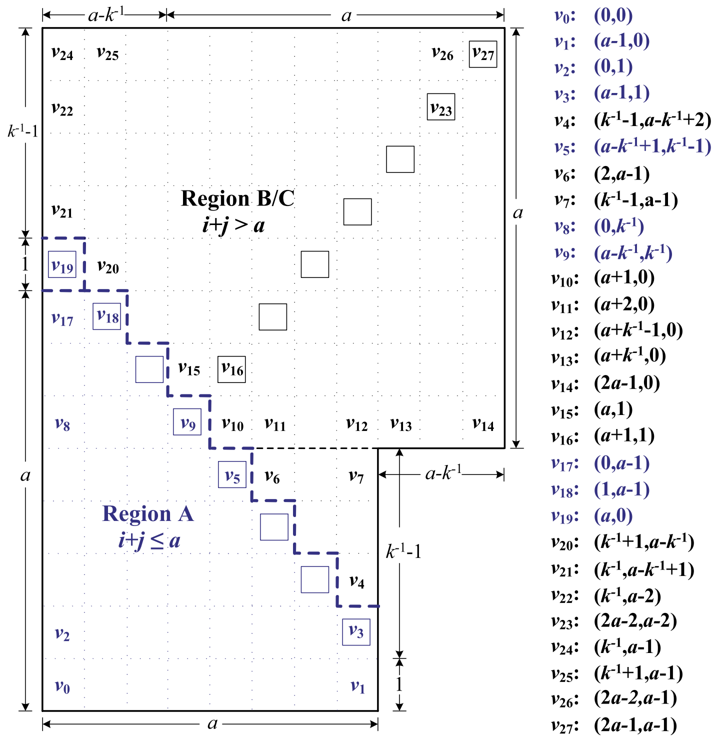

Fig. 12. A framework for layout of $\mathcal{C}_{2a^2}(1, 2ka-1)$, $k \geq 2$.

It is not difficult to show that there exist four vertex-disjoint paths between every pair of distinct vertices in the RTT. For obvious reasons, we exclude those paths that include an incompatible edge. In the process, the number of such paths is not always equal to four.

Vertex transitivity of the RTT allows us to present all paths relative to the fixed vertex (0, 0). There are a total of eleven cases. Fig. 13 distinguishes them in respect of the 14 × 7 RTT. At least one path in each case is necessarily a shortest path while each of the remaining is at most twice as long. (The "dotted" lines in Fig. 13 are meant to delineate various segments of the graph—they do not belong to the graph itself.)

Table 2
Achieving aspect ratio close to unity ($k \geq 2$).

a	k	k^{-1}	Aspect ratio
odd	2	$\frac{1}{2}(a+1)$	$\frac{3a-1}{3a+1}$
$4i$	$\frac{1}{2}(a-2)$	$\frac{1}{2}(a-2)$	$\frac{3a+2}{3a-2}$
$8i+2$	$\frac{1}{4}(a+2)$	$\frac{1}{2}(a+4)$	$\frac{3a-4}{3a+4}$
$8i+6$	$\frac{1}{4}(a-2)$	$\frac{1}{2}(a-4)$	$\frac{3a+4}{3a-4}$

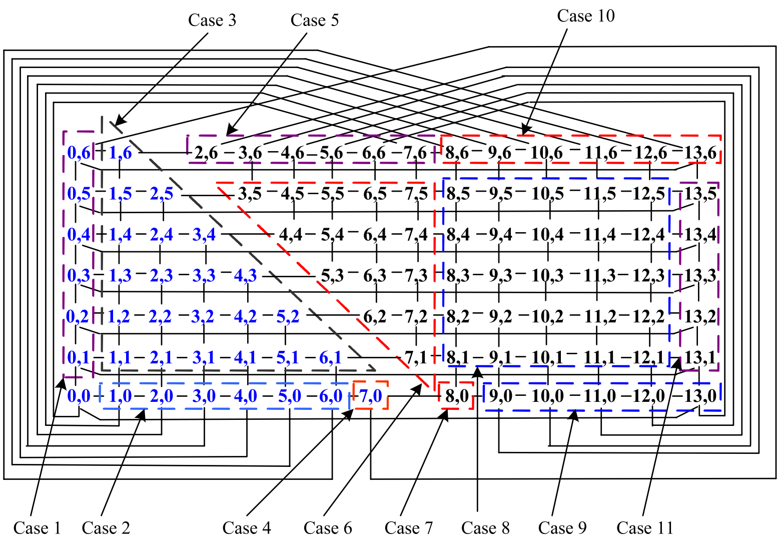

Fig. 13. Various cases in building disjoint paths in the RTT.

Remark. Based on the discussion in Section 3, a distinction is made between (i) $\mathcal{C}_{2a^2}(1, 2ka-1), k = 1$, and (ii) $\mathcal{C}_{2a^2}(1, 2ka-1), k \geq 2$. In particular, a path prefaced with the asterisk contains an edge of the form $(a-i, i)$ that is compatible in respect of the former, but incompatible in respect of the latter.

Case 1: $(0, 0)$ to $(0, j)$, $1 \leq j \leq a-1$

$$\underbrace{(0,0) - (0,1) - \cdots - (0,j)}$$
$$\underbrace{(0,0) - \cdots - (a,0)} - \underbrace{(0,a-1) - \cdots - (0,j)}$$
$$(0,0) - \underbrace{(2a-1,0) - \cdots - (2a-1,j)} - (0,j)$$
$$*(0,0) - \underbrace{(a,a-1) - \cdots - (a,j)} - \underbrace{(a-1,j) - \cdots - (0,j)}.$$

Resp. path lengths: $j, 2a-j, j+2, 2a-j$.

Case 2: $(0, 0)$ to $(i, 0)$, $1 \leq i \leq a-1$

$$\underbrace{(0,0) - (1,0) - \cdots - (i,0)}$$
$$(0,0) - \underbrace{(0,1) - \cdots - (i,1)} - (i,0)$$
$$(0,0) - \underbrace{(a,a-1) - \cdots - (a+i,a-1)} - (i,0)$$
$$*(0,0) - \underbrace{(2a-1,0) - (2a-2,0) - \cdots - (i,0)}.$$

Resp. path lengths: $i, i+2, i+2, 2a-i$.

Case 3: $(0, 0)$ to (i, j), $i+j \leq a$; $i \geq 1$ and $j \geq 1$

$$\underbrace{(0,0) - \cdots - (i,0)} - \underbrace{(i,1) - \cdots - (i,j)}$$
$$\underbrace{(0,0) - (0,1) - \cdots - (0,j)} - \underbrace{(1,j) - \cdots - (i,j)}$$
$$*(0,0) - \underbrace{(a,a-1) - \cdots - (a,j)} - \underbrace{(a-1,j) - \cdots - (i,j)}.$$

Resp. path lengths: $i+j, i+j, 2a-(i+j)$.

Case 4: $(0, 0)$ to $(a, 0)$

$$\underbrace{(0,0)-(1,0)-\cdots-(a,0)}$$
$$\underbrace{(0,0)-(0,1)-\cdots-(0,a-1)}-(a,0)$$
$$*(0,0)-\underbrace{(2a-1,0)-(2a-2,0)-\cdots-(a,0)}.$$

Resp. path lengths: a, a, a.

Case 5: $(0, 0)$ to $(i, a-1)$, $2 \le i \le a$

$$(0,0)-\underbrace{(a,a-1)-(a-1,a-1)\cdots-(i,a-1)}$$
$$(0,0)-\underbrace{(2a-1,0)-(2a-2,0)-\cdots-(a+i,0)}-(i,a-1)$$
$$*\underbrace{(0,0)-\cdots-(0,a-1)}-\underbrace{(1,a-1)-\cdots-(i,a-1)}.$$

Resp. path lengths: $a-i+1, a-i+1, a+i-1$.

Case 6: $(0, 0)$ to (i, j), $3 \le i \le a$; $1 \le j \le a-2$; $i+j \ge a+1$

$$(0,0)-\underbrace{(a,a-1)-\cdots-(a,j)}-\underbrace{(a-1,j)-\cdots-(i,j)}$$
$$(0,0)-\underbrace{(2a-1,0)-\cdots-(a+i,0)}-\underbrace{(i,a-1)-\cdots-(i,j)}$$
$$*\underbrace{(0,0)-(0,1)-\cdots-(0,j)}-\underbrace{(1,j)-\cdots-(i,j)}.$$

Resp. path lengths: $2a-(i+j), 2a-(i+j), i+j$.

Case 7: $(0, 0)$ to $(a+1, 0)$

$$(0,0)-(0,1)-\underbrace{(2a-1,1)-\cdots-(a+1,1)}-(a+1,0)$$
$$(0,0)-\underbrace{(2a-1,0)-(2a-2,0)-\cdots-(a+1,0)}$$
$$*\underbrace{(0,0)-(1,0)-\cdots-(a+1,0)}.$$

Resp. path lengths: $a+1, a-1, a+1$.

Case 8: $(0, 0)$ to (i, j), $a+1 \le i \le 2a-2$ and $1 \le j \le a-2$

$$\underbrace{(0,0)-\cdots-(i-a,0)}-\underbrace{(i,a-1)-\cdots-(i,j)}$$
$$(0,0)-\underbrace{(a,a-1)-\cdots-(a,j)}-\underbrace{(a+1,j)-\cdots-(i,j)}$$
$$\underbrace{(0,0)-\cdots-(0,j)}-\underbrace{(2a-1,j)-(i,j)}$$
$$(0,0)-\underbrace{(2a-1,0)-\cdots-(i,0)}-\underbrace{(i,1)-\cdots-(i,j)}.$$

Resp. path lengths: $i-j, i-j, 2a-(i-j), 2a-(i-j)$.

Case 9: $(0, 0)$ to $(i, 0)$, $a+2 \le i \le 2a-1$

$$(0,0)-(0,1)-\underbrace{(2a-1,1)-(2a-2,1)-\cdots-(i,1)-(i,0)}$$
$$(0,0)-\underbrace{(2a-1,0)-(2a-2,0)-\cdots-(i,0)}$$
$$(0,0)-\underbrace{(a,a-1)-(a-1,a-1)\cdots-(i-a,a-1)}-(i,0)$$
$$*\underbrace{(0,0)-(1,0)-\cdots-(i,0)}.$$

Resp. path lengths: $2a+2-i, 2a-i, 2a+2-i, i$.

Case 10: $(0, 0)$ to $(i, a-1)$, $a+1 \le i \le 2a-1$

$$\underbrace{(0,0)-(1,0)-\cdots-(i-a,0)}-(i,a-1)$$
$$\underbrace{(0,0)-\cdots-(0,a-1)}-\underbrace{(2a-1,a-1)-\cdots-(i,a-1)}$$
$$(0,0)-\underbrace{(a,a-1)-\cdots-(i,a-1)}$$
$$(0,0)-\underbrace{(2a-1,0)-\cdots-(i,0)}-\underbrace{(i,1)-\cdots-(i,a-1)}.$$

Resp. path lengths: $i-a+1, 3a-i-1, i-a+1, 3a-i-1$.

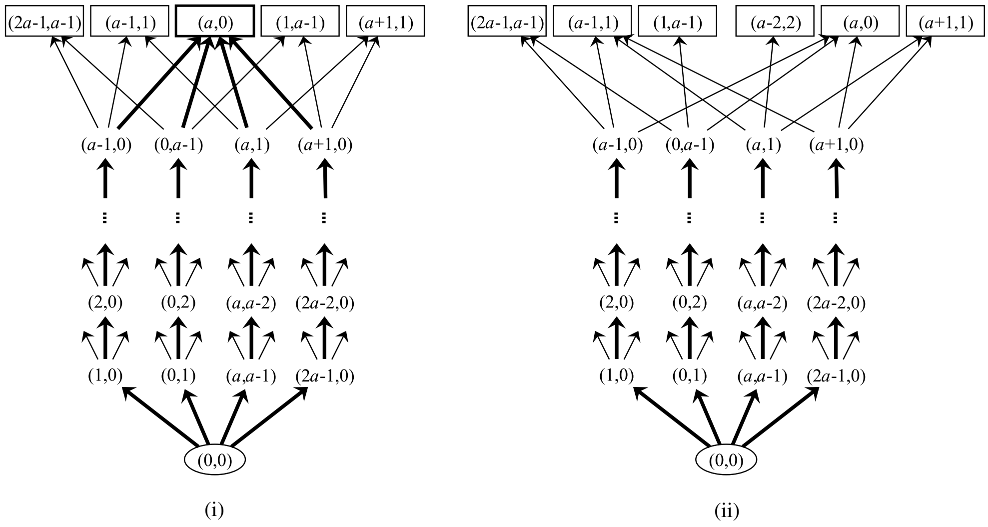

Fig. 14. Essential structures of (i) $2a \times a$ RTT and (ii) $\mathcal{C}_{2a^2}(1, 2a-1)$.

Case 11: $(0, 0)$ to $(2a-1, j)$, $1 \le j \le a-2$

$$\underbrace{(0,0) - \cdots - (0,j)} - (2a-1,j)$$
$$(0,0) - \underbrace{(2a-1,0) - \cdots - (2a-1,j)}$$
$$\underbrace{(0,0) - \cdots - (a-1,0)} - \underbrace{(2a-1,a-1) - \cdots - (2a-1,j)}$$
$$(0,0) - \underbrace{(a,a-1) - \cdots - (a,j)} - \underbrace{(a+1,j) - \cdots - (2a-1,j)}.$$

Resp. path lengths: $j+1, j+1, 2a-1-j, 2a-1-j$.

6. Non-isomorphism

We prove in this section that (1) the circulants constructed in Section 3 are mutually nonisomorphic, and (2) each is nonisomorphic also to the $2a \times a$ RTT. Whereas (1) turns out to be easy, (2) involves some amount of careful work. Meanwhile we continue to use the vertex set of the $2a \times a$ RTT, viz., $\{(i, j) : 0 \le i \le 2a-1 \text{ and } 0 \le j \le a-1\}$ as the vertex set of each of the circulants as well.

Lemma 6.1. *If $s_1 \ne s_2$, $s_1 \ne n - s_2$, and $s_1 s_2 \not\equiv \pm 1 (\bmod n)$, then $\mathcal{C}_n(1, s_1) \not\cong \mathcal{C}_n(1, s_2)$* [12]. ■

Theorem 6.2. *For $a \ge 3$, if $k_1, k_2 \in \{1, \ldots, \lfloor \frac{1}{2}(a-1) \rfloor\}$ and $k_1 \ne k_2$, then $\mathcal{C}_{2a^2}(1, 2k_1 a - 1)$ and $\mathcal{C}_{2a^2}(1, 2k_2 a - 1)$ are not isomorphic.*

Proof. Let a, k_1 and k_2 be as stated, and $k_1 < k_2$. Further, let $s_1 = 2k_1 a - 1$, $s_2 = 2k_2 a - 1$ and $n = 2a^2$. It is clear that $2a - 1 \le s_1 < s_2 < \frac{1}{2} n$. Therefore, $s_1 \ne n - s_2$ and $s_2 \ne n - s_1$. Further, $s_1 s_2 = 4k_1 k_2 a^2 - 2(k_1 + k_2)a + 1$ that reduces to $2a^2 - 2(k_1 + k_2)a + 1$ modulo n. Notice that $1 < k_1 + k_2 < a$. Accordingly, $s_1 s_2 \not\equiv \pm 1 (\bmod n)$. The claim then follows by Lemma 6.1. ■

6.1. *A distinguishing characteristic of the $2a \times a$ RTT*

Consider the vertex partition $\{V_0, \ldots, V_a\}$ of the RTT, where V_k consists of vertices at a distance of k from $(0, 0)$, $0 \le k \le a$, cf. Section 2. Call a vertex u a *predecessor* of v if $u \in V_{k-1}$, $v \in V_k$, and u and v are adjacent, where $1 \le k \le a$. Use the term *successor* in a natural way.

Fact 1. 1. *There are four disjoint shortest paths of length a each that originate at $(0, 0)$ and converge at a unique vertex at the diametrical level.*

2. *Each of the foregoing paths, say, $(0, 0) - (u_1, v_1) - \cdots - (u_{a-1}, v_{a-1}) - (u_a, v_a)$ is such that the vertex (u_d, v_d) has a single predecessor and three successors, where $1 \le d \le a-1$.*
3. *None of the remaining vertices at levels $1, \ldots, a-1$ has the foregoing property of having a single predecessor and three successors.* ■

Fig. 14(i) illustrates Fact 1. The vertices on the respective paths at the dth level are $(d, 0)$, $(0, d)$, $(a, a-d)$ and $(2a-d, 0)$, $1 \le d \le a-1$. Further, the nodes $(a-1, 0)$, $(0, a-1)$, $(a, 1)$ and $(a+1, 0)$ at the $(a-1)$th level have between them a total of five neighboring vertices at the ath level: $(2a-1, a-1)$, $(a-1, 1)$, $(a, 0)$, $(1, a-1)$ and $(a+1, 1)$.

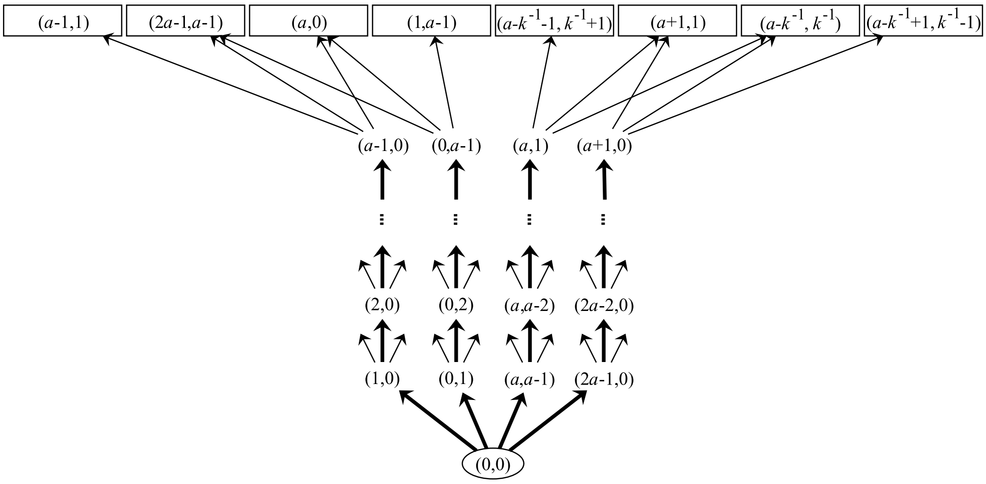

Fig. 15. The essential structure of $\mathcal{C}_{2a^2}(1, 2ka - 1)$, $k \geq 2$.

Table 3
A comparison of $\mathcal{C}_{2a^2}(1,\ 2ka-1)$ and $\mathcal{C}_{2a^2}(a-1,\ a)$.

	$\mathcal{C}_{2a^2}(1,\ 2ka-1)$	$\mathcal{C}_{2a^2}(a-1,\ a)$
Bipartite?	Yes	No
Diameter	a	a
Average distance	$\frac{2}{3}a$ (approx.)	$\frac{2}{3}a$ (approx.)
Node distribution (level diagram)	$1+\underbrace{4d}_{1 \leq d \leq a-1}+2a-1$	$1+\underbrace{4d}_{1 \leq d \leq a-1}+2a-1$
Layout	L-shaped	Rectangular
Aspect ratio	Between $\frac{1}{2}$ and 2	2

$2a \times a$ RTT vs. $\mathcal{C}_{2a^2}(1, 2ka - 1)$: The circulants derived from the RTT and the RTT itself are all vertex transitive, and their vertex sets are assumed (without loss of generality) to be the same, so their characteristics may be examined relative to the fixed node (0, 0).

Fig. 14(ii) presents the structure of $\mathcal{C}_{2a^2}(1, 2a - 1)$ that is analogous to that of the RTT appearing in Fig. 14(i). Everything stays intact up to the $(a-1)$th level. Further, the nodes of the four disjoint paths at the $(a-1)$th level are together adjacent to a total of six nodes at the ath level. However, the paths themselves do not collectively converge at any one of those six nodes.

It follows that Facts 1(2) and 1(3) continue to hold in respect of $\mathcal{C}_{2a^2}(1, 2a-1)$ while Fact 1(1) does not hold. An identical conclusion is reached if $k \geq 2$. See Fig. 15.

Theorem 6.3. *The $2a \times a$ RTT and the circulants $\mathcal{C}_{2a^2}(1, 2ka - 1)$, $k \geq 1$, are mutually non-isomorphic.* ■

Remark. Theorem 6.3 suggests that the $2a \times a$ RTT itself is probably not a circulant graph.

7. Concluding remarks

This paper deals with the routing in the bipartite circulants $\mathcal{C}_{2a^2}(1, 2ka - 1)$, $k \geq 1$, devised by Tzvieli [30] in 1991. The details are precise enough to warrant an easy implementation.

The study critically relies on the structural similarity between the $2a \times a$ rectangular twisted torus (RTT) and $\mathcal{C}_{2a^2}(1, 2ka-1)$. The advantage is that the routing, which is otherwise challenging in the case of a circulant, becomes feasible and intuitive.

Additional results include a set of vertex-disjoint paths between every pair of distinct vertices in the RTT that map into analogous paths in $\mathcal{C}_{2a^2}(1, 2ka - 1)$, thus strengthening the fault tolerance and communication capability of the circulants.

Among other circulants in the literature, $\mathcal{C}_{2a^2}(a-1,\ a)$ is one, which is known to be optimal [3] for a long time. Since the circulants in the present paper are also on $2a^2$ vertices, it is instructive to compare the two. To that end, Table 3 presents certain relevant characteristics of $\mathcal{C}_{2a^2}(1,\ 2ka-1)$ and $\mathcal{C}_{2a^2}(a-1,\ a)$.

It seems that the methodology used in the present paper will be applicable to other families of four-regular circulants obtainable from variants of the rectangular twisted torus.

Acknowledgments

Thanks to Dr. Brian Alspach and Dr. Jonathan D.H. Smith for the encouragement, and to the referee for remarks that improved the presentation. The work itself has been partially supported by the St. Cloud State University Researchers Fund.

References

[1] B. Alspach, August 2011, personal communication.
[2] B. Alspach, T.D. Parsons, Isomorphism of circulant graphs and digraphs, Discrete Math. 25 (1979) 97–108.
[3] R. Beivide, E. Herrada, J.L. Balcázar, A. Arruabarrena, Optimal distance networks of low degree for parallel computers, IEEE Trans. Comput. 40 (10) (1991) 1109–1124.
[4] J.-C. Bermond, F. Comellas, D.F. Hsu, Distributed loop computer networks: a survey, J. Parallel Distrib. Comput. 24 (1995) 2–10.
[5] F. Boesch, R. Tindell, Circulants and their connectivities, J. Graph Theory 8 (1984) 487–499.
[6] F. Boesch, J.F. Wang, Reliable circulant networks with minimum transmission delay, IEEE Trans. Circuits Syst. CAS-32 (1985) 1286–1291.
[7] W.J. Bouknight, S.A. Denenberg, D.E. McIntyre, J.M. Randall, A.H. Sameh, D.L. Slotnick, The illiac IV system, Proc. IEEE 60 (4) (1972) 369–388.
[8] I. Broere, J.H. Hattingh, Products of circulant graphs, Quaest. Math. 13 (1990) 191–216.
[9] J.-Y. Cai, G. Havas, B. Mans, A. Nerurkar, J.-P. Seifert, I. Shparlinski, On routing in circulant graphs, in: Computing and Combinatorics, in: LNCS, vol. 1627, 1999, pp. 360–369.
[10] J.M. Cámara, M. Moretó, E. Vallejo, R. Beivide, J. Miguel-Alonso, C. Martínez, J. Navaridas, Twisted torus topologies for enhanced interconnection networks, IEEE Trans. Parallel Distrib. Syst. 21 (12) (2010) 1765–1778.
[11] T. Dobravec, J. Žerovnik, B. Rovič, An optimal message routing algorithm for circulant networks, J. Syst. Archit. 52 (2006) 298–306.
[12] F. Gobel, N.A. Neutel, Cyclic graphs, Discrete Appl. Math. 99 (2000) 3–12.
[13] R. Hammack, W. Imrich, S. Klavžar, Handbook of Product Graphs, second ed., CRC Press, Boca Raton, FL, 2011.
[14] H.A. Harutyunyan, E. Maraachlian, Broadcasting in optimal bipartite double loop graphs, in: Proc. 10th International Conf. Information Visualization, London, 2006, pp. 521–528.
[15] C. Heuberger, On planarity and colorability of circulant graphs, Discrete Math. 268 (2003) 153–169.
[16] M.C. Heydemann, Cayley graphs and interconnection networks, in: G. Hahn, G. Sabidussi (Eds.), Graph Symmetry, Kluwer Acad. Publishing, Dordrecht, 1997, pp. 167–224.
[17] D.F. Hsu, On container width and length in graphs, groups and networks, IEICE Trans. Fundam. Electron. Commun. Comput. Sci. E77-A (1994) 668–680.
[18] D.F. Hsu, T. Łuczak, On the k-diameter of k-regular k-connected graphs, Discrete Math. 133 (1994) 291–296.
[19] F.K. Hwang, A survey on multi-loop networks, Theoret. Comput. Sci. 299 (2003) 107–121.
[20] P.K. Jha, R. Prasad, Hamiltonian decomposition of the rectangular twisted torus, IEEE Trans. Parallel Distrib. Syst. 23 (8) (2012) 1504–1507.
[21] F.C.M. Lau, G. Chen, Optimal layouts of midimew networks, IEEE Trans. Parallel Distrib. Syst. 7 (9) (1996) 954–961.
[22] F.T. Leighton, Introduction to Parallel Algorithms and Architectures: Arrays, Trees, Hypercubes, Morgan-Kaufmann, 1992.
[23] C. Martínez, R. Beivide, E.M. Gabidulin, Perfect codes for metrics induced by circulant graphs, IEEE Trans. Inform. Theory 53 (9) (2007) 3042–3052.
[24] C. Martínez, R. Beivide, E. Stafford, M. Moretó, E.M. Gabidulin, Modeling toroidal networks with the Gaussian integers, IEEE Trans. Comput. 57 (8) (2008) 1046–1056.
[25] C. Martínez, E. Vallejo, R. Beivide, C. Izu, M. Moreto, Dense Gaussian networks: suitable topologies for on-chip multiprocessors, Int. J. Parallel Program. 34 (3) (2006) 193–211.
[26] D. Medhi, K. Ramasamy, Network Routing: Algorithms, Protocols, and Architectures, Morgan Kaufmann, 2007.
[27] M. Muzychuk, Adam's conjecture is true in the square-free case, J. Combin. Theory Ser. A 72 (1995) 118–134.
[28] S. Nicoloso, U. Pietropaoli, Isomorphism testing for circulant graphs $\mathcal{C}_n(a, b)$, http://www.optimization-online.org/DB_FILE/2010/03/2577.pdf.
[29] S.-M. Tang, Y.-L. Wang, C.-Y. Li, Generalized recursive circulant graphs, IEEE Trans. Parallel Distrib. Syst. 23 (1) (2012).
[30] D. Tzvieli, Minimal diameter double-loop networks-I: large infinite optimal families, Networks 21 (1991) 387–415.
[31] C.K. Wong, D. Coppersmith, A combinatorial problem related to multimodule memory organization, J. ACM 21 (3) (1974) 392–402.
[32] J. Žerovnik, T. Pisanski, Computing the diameter in multiple-loop networks, J. Algorithms 14 (1993) 226–243.